JOURNAL OF Materials CHEMISTRY

Electrodeposition of lead selenide thin films

Heini Saloniemi,*[a] Tapio Kanniainen,†[a] Mikko Ritala,[a] Markku Leskelä[a] and Reijo Lappalainen[b]

[a]*Department of Chemistry, P.O. Box 55, FIN-00014 University of Helsinki, Finland*

[b]*Accelerator Laboratory, University of Helsinki, P.O. Box 9, FIN-00014 Helsinki, Finland*

PbSe thin films have been electrodeposited potentiostatically from aqueous solutions containing lead complexed with EDTA (ethylenediaminetetraacetic acid) and SeO_2. The effects of deposition parameters such as deposition potential, concentrations of source materials and current density were studied. Cyclic voltammetry was used for studying the film deposition reactions and for finding the appropriate deposition potential range. The films were characterized by X-ray diffraction (XRD), energy dispersive X-ray spectroscopy (EDX), scanning electron microscopy (SEM), Rutherford backscattering spectrometry (RBS), elastic recoil detection analysis (ERDA), deuteron induced reactions and profilometry. Nearly stoichiometric, smooth, mirror-like PbSe films were obtained at deposition potentials between −0.6 and −0.8 V *vs.* saturated calomel electrode (SCE) when the concentration of lead was ten times higher than the concentration of selenium, and between −0.4 and −0.75 V *vs.* SCE when the lead excess was a hundred-fold.

Lead chalcogenides (PbS, PbSe, PbTe) are interesting narrow band gap semiconductors. These photoconductors have widely been studied, for example, for IR detector applications.[1] Thin films of PbSe, which has the narrowest band gap of the lead chalcogenides, have been grown by various methods including chemical bath deposition,[2] molecular beam epitaxy,[3] vacuum deposition,[4] successive ionic layer adsorption and reaction technique[5] and electrodeposition.[6]

Electrodeposition is a simple and low cost thin film deposition method with many advantages,[7] for example, substrates of variable sizes and shapes can be used. The deposition process can be controlled more accurately and the reactions involved are closer to equilibrium than in many gas phase methods. Unlike chemical gas phase methods, electrochemical deposition does not involve the use of toxic gaseous precursors.[7] On the other hand, in comparison with chemical bath deposition (CBD), the preparation of the deposition solution for the electrochemical method is simpler since no strict control of the oxidation state of the selenium precursor is required. Several chalcogenides have been electrodeposited, for example sulfides CdS,[8] SnS,[8] Bi_2S_3,[9] Sb_2S_3,[9] As_2S_3,[9] YS_x,[10] MoS_2[11] and PbS,[12] selenides CdSe,[13] PbSe,[6] ZnSe,[14] InSe,[15] YSe_2,[10] $Zn_{1-x}Cd_xSe$[16] and $CuInSe_2$,[17] and tellurides CdTe,[18,19] ZnTe,[20] YTe_x[10] and Bi_2Te_3.[21]

In this work, electrodeposition of PbSe thin films has been examined. Earlier Molin and Dikusar[6] electrodeposited PbSe from solutions where the concentration ratios [Se]/[Pb] were within a range of 0.2–11. They obtained stoichiometric films only when the concentration ratio was close to 0.5. The present work is based on a different approach which makes use of induced codeposition. According to the thermodynamic analysis of Kröger[22] PbSe belongs to the same group as CdSe and CdTe. These compounds can be electrodeposited at a potential between the deposition potentials of their constituents. This means that the deposition of the more noble component, which in the case of PbSe is selenium, induces the deposition of the less noble component, *i.e.* lead. In other words, the reduction and deposition of lead on selenium occurs at more positive potential than on itself. Therefore stoichiometric PbSe films should be obtained if the substrate potential is kept between the deposition potentials of pure lead and selenium, and if the concentration of lead is much higher than that of selenium.[22] Under such conditions the film stoichiometry is rather insensitive to unavoidable small variations in precursor concentrations. In the first part of this work, cyclic voltammetry was used in order to study the film deposition reactions and to find a suitable electrodeposition potential region for PbSe, and in the second part thin films were grown and characterized.

Experimental

The solutions used contained dissolved SeO_2 (May and Baker), $Pb(CH_3CO_2)_2$ (Riedel de Häen p.a.) and EDTA disodium salt (Baker p.a.) in deionized water. Within the pH range used selenium is expected to be in the form of $HSeO_3^-$.[23] EDTA was used to complex Pb in order to prevent the spontaneous precipitation of insoluble $PbSeO_3$. In cyclic voltammetry measurements, $HSeO_3^-$ concentrations were varied from 0.0001 to 0.1 M. Lead acetate concentrations were within 0.001–0.1 M with a slight excess of EDTA. The pH of the solution was adjusted with CH_3CO_2H and NaOH. Thin films were deposited from solutions containing 0.001 M $HSeO_3^-$, 0.1 or 0.01 M $Pb(CH_3CO_2)_2$ and 0.13 or 0.013 M EDTA, respectively. The films were grown at the natural pH of the solution which was *ca.* 3.4.

Both the cyclic voltammetry measurements and electrodeposition of the PbSe films were carried out using a Metrohm 626 potentiostat and a three-electrode cell. The electrodes were an SnO_2 coated glass substrate as a working electrode, a graphite rod as a counter electrode and a saturated calomel electrode (SCE) as the reference electrode. The substrates were cleaned ultrasonically in water and ethanol before use. In cyclic voltammetry the voltage scan rate was 100 mV s^{-1}. Both electrodeposition and cyclic voltammetry studies were carried out at room temperature and from unstirred solutions unless otherwise stated.

The crystal structure and orientation of the films were examined by a Philips MPD 1880 powder X-ray diffractometer using Cu-Kα radiation. Surface morphologies of the films were studied by a Zeiss DSM 926 scanning electron microscope (SEM). Chemical compositions and thicknesses of the films were measured by a Link ISIS energy dispersive X-ray spectrometer (EDX) which was installed to the SEM equipment. A GMR electron probe thin film microanalysis program[24] was used to analyse the EDX results. Some films were also characterized by Rutherford backscattering spectrometry (RBS), deuteron induced reactions and elastic recoil detection analysis

† Present address: Microchemistry Ltd, P.O. Box 45, FIN-02151 Espoo, Finland.

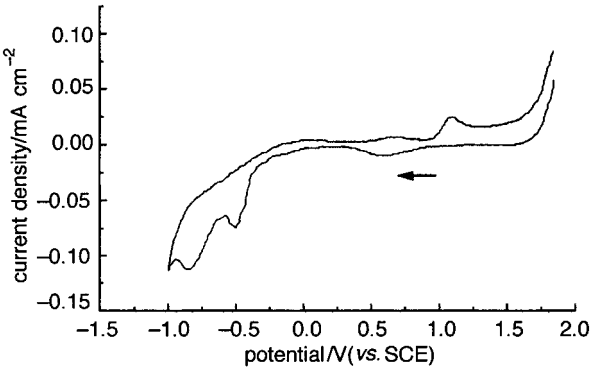

Fig. 1 Cyclic voltammogram for a SnO_2 electrode in a solution containing 0.006 M $HSeO_3^-$. Scan rate = 100 mV s^{-1}.

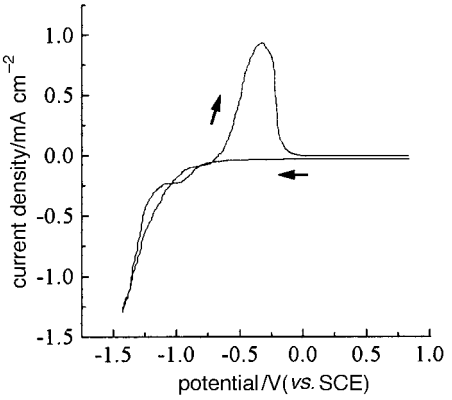

Fig. 2 Cyclic voltammogram for a SnO_2 electrode in a solution containing 0.001 M $Pb(CH_3CO_2)_2$ complexed with EDTA. Scan rate = 100 mV s^{-1}.

(ERDA) using $^4He^+$ and $^2H^+$ ions from the 2.4 MV Van de Graaff accelerator at the Accelerator Laboratory. Film thicknesses were also measured by a Dektak profilometer.

Results and Discussion

Cyclic voltammetry

Cyclic voltammetry was used to monitor the electrochemical reactions in solutions of $Pb(CH_3CO_2)_2$, Pb^{2+} complexed with EDTA [$Pb(EDTA)^{2-}$], $HSeO_3^-$, and mixtures, in order to find the suitable PbSe deposition potential range. All voltammetry curves were scanned first in the cathodic direction and the negative current density indicates a cathodic current.

Fig. 1 shows a cyclic voltammogram of a solution containing 0.006 M $HSeO_3^-$ in acetic acid at pH 3.8. Two reduction waves are clearly observed at potentials of −0.5 and −0.8 V *vs.* SCE. These reduction waves are expected to be due to the irreversible reactions (1) and (2).[14]

$$HSeO_3^-(aq) + 5H^+(aq) + 4e^- \rightarrow Se(s) + 3H_2O \quad (1)$$

$$Se(s) + 2H^+(aq) + 2e^- \rightarrow H_2Se(aq) \quad (2)$$

The corresponding oxidation waves can be seen at potentials of 0.6 [eqn. (2)] and 1.1 V [eqn. (1)] *vs.* SCE. At a potential of 1.5 V *vs.* SCE oxygen evolution commences. The formation of elemental selenium was evidenced by holding the substrate at a constant potential of −0.5 V *vs.* SCE and observing the appearance of a red selenium deposit. In addition to reactions (1) and (2), direct six-electron reduction of the $HSeO_3^-$ ion to H_2Se has also been reported.[13] Furthermore, different reduction potentials, −0.25[16] and −0.4[13] V *vs.* SCE, have also been observed. These differences may be ascribed to different substrates and other measurement conditions, such as stirring, pH and concentration.[13]

In $Pb(CH_3CO_2)_2$ solutions which did not contain EDTA, a nearly reversible reduction of Pb^{2+} occurred at a potential of −0.6 V *vs.* SCE according to reaction (3).

$$Pb^{2+}(aq) + 2e^- \rightleftharpoons Pb(s) \quad (3)$$

When lead was complexed with EDTA, the reduction potential was shifted from −0.6 to −0.8 V *vs.* SCE (Fig. 2). The oxidation potential is *ca.* −0.4 V *vs.* SCE which is the same as measured without complexation. Thus, besides preventing the precipitation of $PbSeO_3$, complexation of lead with EDTA also widens the deposition potential range of PbSe.

A cyclic voltammogram measured after mixing $HSeO_3^-$ and $PbEDTA^{2-}$ solutions is shown in Fig. 3 (solid line). Deposition of PbSe [reactions (1) and (4)] begins at a potential of −0.8 V vs. SCE.

$$Pb(EDTA)^{2-}(aq) + Se(s) + 2H^+(aq) + 2e^- \rightleftharpoons PbSe(s) + H_2EDTA^{2-}(aq) \quad (4)$$

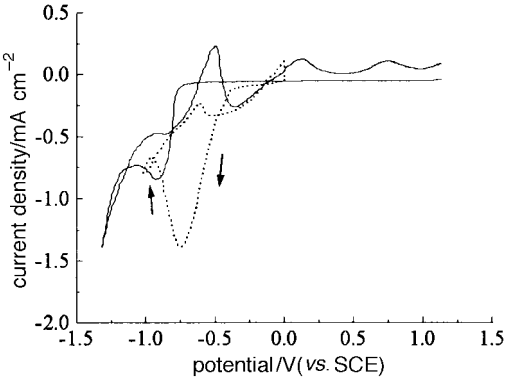

Fig. 3 Cyclic voltammogram in the solution containing 0.01 M $Pb(CH_3CO_2)_2$ complexed with EDTA and 0.001 M $HSeO_3^-$ for a SnO_2 electrode (solid line) and for a PbSe film (dotted line). Scan rate = 100 mV s^{-1}.

The steep rise in the cathodic current at a potential of −1.2 V *vs.* SCE can be attributed to the onset of the formation of elemental lead (*cf.* Fig. 2). The deposition potential of selenium has been shifted compared with pure $HSeO_3^-$ solution (Fig. 1). Similar shifts have been observed for ZnSe, CdTe and ZnTe deposition, and have been attributed to the adsorption site competition between the different precursors.[14,20] The PbSe deposition current is dependent on the concentration of $HSeO_3^-$ which was demonstrated by adding $HSeO_3^-$ and observing a rise in the peak current. On the other hand, increasing the concentration of $Pb(EDTA)^{2-}$ did not have any effect on the current density in the PbSe formation range but, instead, it moved the reduction of lead to more positive potentials. In general, these results are similar to those observed when deposition of CdTe and ZnSe has been studied.[14]

In the reversed scan the first oxidation peak is observed at a potential of −0.5 V *vs.* SCE which is almost the same as that for a solution of pure $Pb(EDTA)^{2-}$ and, thus, it is most likely due to the oxidation of elemental lead. The second anodic wave at a potential of 0.15 V *vs.* SCE must correspond to the oxidation of PbSe [eqn. (4)] because it was not observed in either of the pure solutions (Fig. 1 and 2). The anodic wave at a potential of 0.75 V *vs.* SCE depicts oxidation of selenium. The hysteresis observed in the region from −0.1 to −0.8 V *vs.* SCE indicates that the PbSe deposition occurs more readily on a PbSe surface than on a clean SnO_2 surface.

The dotted line in Fig. 3 depicts the voltammogram measured after deposition of PbSe film, *i.e.* the working electrode was actually lead selenide instead of SnO_2. It can be seen that besides PbSe, lead is also deposited at a more positive potential on the PbSe surface (−0.8 V *vs.* SCE) than on the SnO_2 surface (−1.0 V *vs.* SCE). Altogether the above results lead into a

conclusion that with these source concentrations stoichiometric PbSe can be deposited between potentials of −0.1 and −0.8 V *vs.* SCE.

So far it has been assumed that formation of PbSe occurs *via* underpotential deposition of lead according to reaction (4). On the other hand, for CdTe alternative reactions, analogous to reactions (5) and (6), have been stated.[19] At this stage, however, it is very difficult to distinguish which actually occur.

$$Pb(EDTA)^{2-}(aq) + H_2Se(aq) \rightleftharpoons PbSe(s) + H_2EDTA^{2-}(aq) \quad (5)$$

$$Pb(s) + Se(s) \rightleftharpoons PbSe(s) \quad (6)$$

Film growth

Lead selenide films were deposited at various potentials at two different $Pb(EDTA)^{2-}$ concentrations: 0.1 and 0.01 M. The concentration of $HSeO_3^-$ was 0.001 M in both cases. For both $Pb(EDTA)^{2-}$ concentrations, current densities during deposition at potentials more negative than −0.5 V *vs.* SCE stabilized within a few min to *ca.* 0.15 mA cm^{-2}. However, at potentials more positive than −0.5 V *vs.* SCE, the film growth rates were very slow, and at these potentials magnetic stirring was employed to speed up the deposition. At potentials more positive than −0.4 V *vs.* SCE films were not deposited at all. Film thicknesses were determined by EDX, RBS and profilometry which gave fairly consistent results. After deposition for 1 h the film thicknesses were *ca.* 0.25 μm, while beyond this time the films peeled off from the substrate.

The deposition potential employed significantly affected the film compositions. Fig. 4 shows compositions measured by EDX for films deposited at different potentials. When the $Pb(EDTA)^{2-}$ concentration was 0.01 M, PbSe films with constant composition could be deposited between potentials of −0.6 and −0.8 V *vs.* SCE [Fig. 4(*a*)]. The excess of lead in

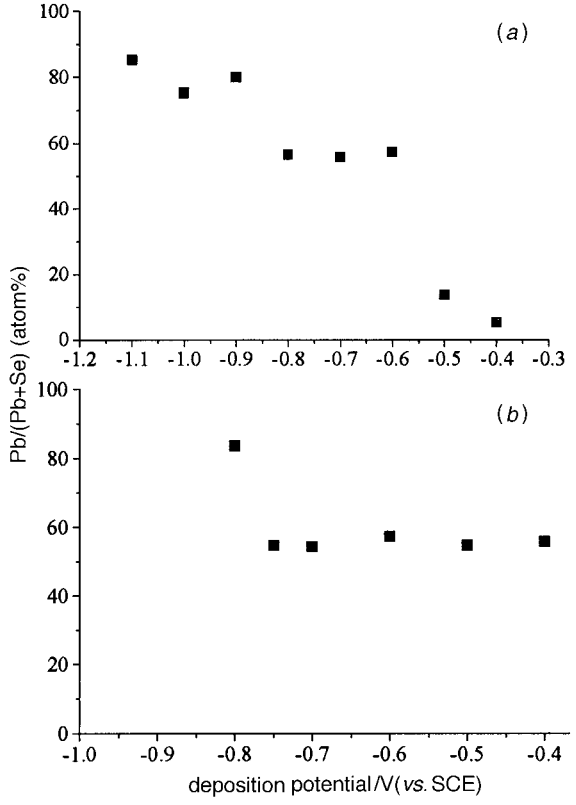

Fig. 4 (*a*) The Pb/(Pb + Se) ratio measured by EDX for films deposited at different potentials. The $Pb(EDTA)^{2-}$ concentration in the deposition solution was 0.01 M. (*b*) Same as (*a*) except that the $Pb(EDTA)^{2-}$ concentration in the deposition solution was 0.1 M.

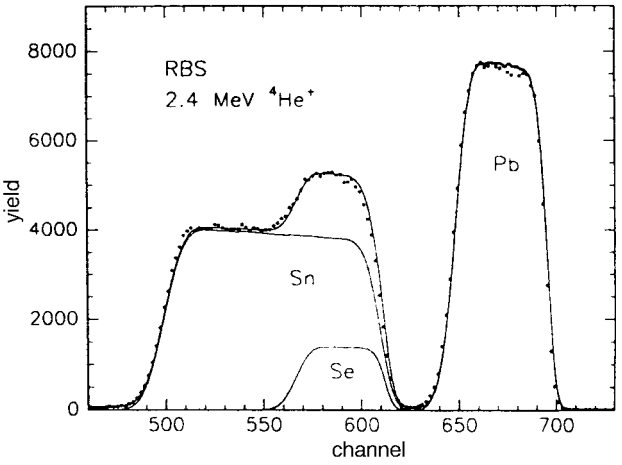

Fig. 5 An RBS spectrum of a PbSe thin film on SnO_2/glass substrate (points) together with the theoretical computer simulation for a film with a composition of Pb:Se:O:H = 0.37:0.37:0.12:0.14 (solid line). Also signals corresponding to Pb, Se and Sn are separately shown.

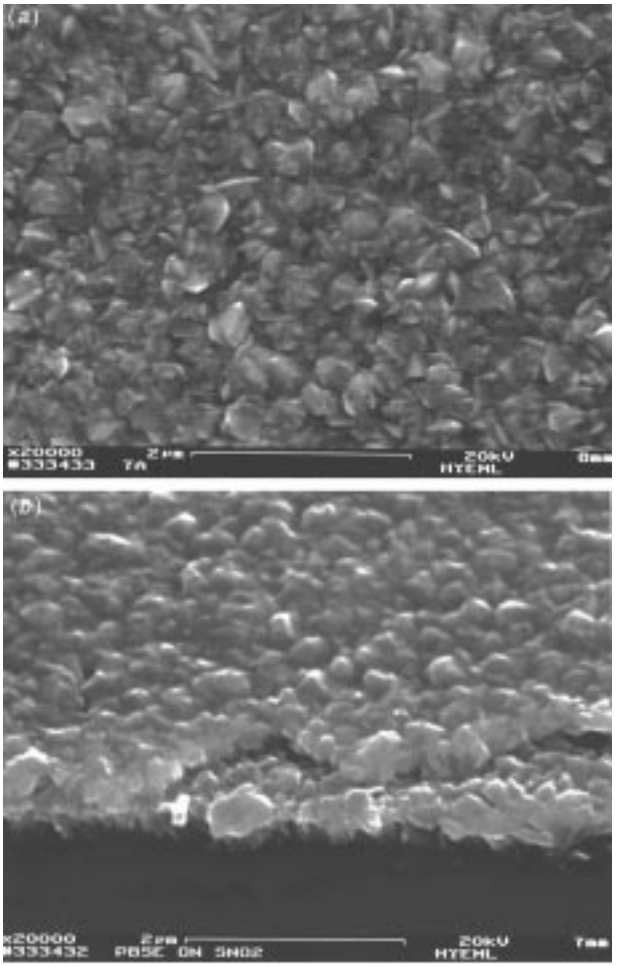

Fig. 6 (*a*) SEM image of the top view of an electrodeposited PbSe thin film. (*b*) SEM image of the fractured cross-section of an electrodeposited PbSe thin film on the top of the SnO_2 film.

films which were deposited at potentials below −0.8 V *vs.* SCE could be seen as dark regions, whereas the excess of selenium obtained at deposition potentials above −0.6 V *vs.* SCE gave a reddish colour. When the films were deposited from 0.1 M $Pb(EDTA)^{2-}$ solutions the region of the constant stoichiometry was broader; from −0.4 to −0.75 V *vs.* SCE [Fig. 4(*b*)]. The potential region where the growth of stoichiometric PbSe

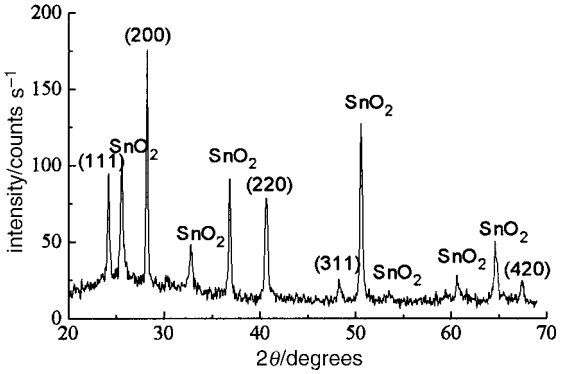

Fig. 7 XRD pattern of an electrodeposited PbSe thin film; the peak indexes refer to cubic PbSe[25]

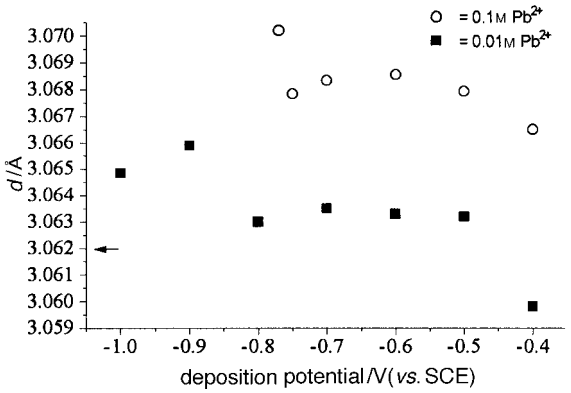

Fig. 8 The *d* values measured by XRD for the (200) reflection of PbSe deposited at different potentials measured by XRD with two different $Pb(EDTA)^{2-}$ concentrations. The arrow indicates the reference value.[25]

film takes place corresponds to the cyclic voltammogram measured after film growth (Fig. 3, dotted line).

Although EDX is a suitable method for routine analysis of thin films, it can be regarded only as semiquantitative and it is not capable of distinguishing between oxygen in the film and in the substrate. Therefore, some representative films were also analysed by RBS (Fig. 5). The samples for RBS were chosen from the potential region where according to the EDX the Pb to Se ratio was nearly constant (Fig. 4). RBS measurements indicated that within this potential region the Pb : Se ratio was 1 : 1. Furthermore, analysis of the RBS spectra indicated that the films contained light-atom impurities such as oxygen. Using deuteron induced reactions, oxygen contents of *ca.* 8–12 atom% were determined, whereas ERDA measurements revealed that the films contained *ca.* 10–14 atom% hydrogen. This results in an overall composition of Pb : Se : O : H = 0.37 : 0.37 : 0.12 : 0.14 which in a simulation of RBS spectrum gives a good fit to the experimental data (Fig. 5). The oxygen and hydrogen residues exist most probably as water and hydroxy groups, although $PbSeO_x$ species may also be present. Obviously, water and hydroxy groups originate from the aqueous deposition solution. To remove water and hydroxy residues from the films, they were annealed under a N_2 atmosphere at 200 °C for 1 h. However, only *ca.* 20% of hydrogen was removed, thereby indicating that water was rather strongly bound to the films.

Stoichiometric PbSe films were mirror-like, smooth and light grey. Fig. 6 shows an SEM image of the top view [Fig. 6(*a*)] and a fractured cross-section [Fig. 6(*b*)] of the PbSe film deposited at a potential of −0.7 V *vs.* SCE. X-Ray diffraction (XRD) measurements showed that all the PbSe films had a polycrystalline, randomly oriented, cubic rock salt structure in their as-deposited state (Fig. 7). The excess of lead obtained at the most negative potentials was found to be crystalline whereas the excess of selenium obtained at the other extreme of deposition potentials was amorphous. XRD also indicated changes in the interplanar distances (*d* values) as a function of deposition potential (Fig. 8). The *d* values of the (200) reflection are a little higher than that in the literature (3.062 Å),[25] especially at higher lead concentrations.

Conclusions

PbSe thin films were electrodeposited potentiostatically from solutions which contained either 0.01 or 0.1 M $Pb(EDTA)^{2-}$ and 0.001 M $HSeO_3^-$. Different deposition potentials were studied and it was observed that nearly stoichiometric films can be deposited with lower lead concentrations between potentials of −0.6 and −0.8 V *vs.* SCE, and with higher lead concentrations between potentials of −0.4 and −0.75 V *vs.* SCE. This potential region was also verified from a cyclic voltammogram measured using a PbSe film as the working electrode. The as-grown films were found to contain hydrogen and oxygen as impurities. The films were polycrystalline and cubic.

Facilities provided by the Department of Electron Microscopy at the University of Helsinki were exploited for SEM characterization. This work was partly supported by the Neste Foundation.

References

1 T. H. Johnson, *Proc. SPIE, Int. Soc. Opt. Eng.*, 1984, **443**, 60.
2 S. Gorer, A. Albu-Yaron and G. Hodes, *Chem. Mater.*, 1995, **7**, 1243.
3 H. Zogg, C. Maissen, J. Masek, T. Hoshino, S. Blunier and A. N. Tiwari, *Semicond. Sci. Technol.*, 1991, **6**, C36.
4 V. Damodara Das and K. Seetharama Bhat, *J. Mater. Sci.*, 1990, **1**, 169.
5 T. Kanniainen, S. Lindroos, J. Ihanus and M. Leskelä, *J. Mater. Chem.*, 1996, **6**, 983.
6 A. N. Molin and A. I. Dikusar, *Thin Solid Films*, 1995, **265**, 3.
7 K. Rajeshwar, *Adv. Mater.*, 1992, **4**, 23.
8 A. Adachi, A. Kudo and T. Sakata, *Bull. Chem. Soc. Jpn.*, 1995, **68**, 3283.
9 N. S. Yesugade, C. D. Lokhande and C. H. Bhosale, *Thin Solid Films*, 1995, **263**, 145.
10 U. K. Mohite and C. D. Lokhande, *Appl. Surf. Sci.*, 1996, **92**, 151.
11 E. A. Ponomarev, M. Neumann-Spallart, G. Hodes and C. Lévy-Clément, *Thin Solid Films*, 1996, **280**, 86.
12 M. Takahashi, Y. Ohishima, K. Nagata and S. Furuta, *J. Electroanal. Chem.*, 1993, **359**, 281.
13 M. Skyllas Kazacos, and B. Miller, *J. Electrochem. Soc.*, 1980, **127**, 869.
14 C. Natarajan, M. Sharon, C. Levy-Clement and M. Neumann-Spallart, *Thin Solid Films*, 1994, **237**, 118.
15 Y. Igasaki and T. Fujiwara, *J. Cryst. Growth*, 1996, **158**, 268.
16 C. Natarajan, G. Nogami and M. Sharon, *Thin Solid Films*, 1995, **261**, 44.
17 R. N. Bhattacharya, *J. Electrochem. Soc.*, 1983, **130**, 2040.
18 M. P. R. Panicker, M. Knaster and F. A. Kröger, *J. Electrochem. Soc.*, 1978, **125**, 566.
19 A. Saraby-Reintes, L. M. Peter, M. E. Örzan, S. Dennison and S. Webster, *J. Electrochem. Soc.*, 1993, **140**, 2880.
20 M. Neumann-Spallart and C. Köningstein, *Thin Solid Films*, 1995, **265**, 33.
21 P. Magri, C. Boulanger and J-M. Lecuire, *J. Mater. Chem.*, 1996, **6**, 773.
22 F. A. Kröger, *J. Electrochem. Soc.*, 1978, **125**, 2028.
23 C. Baes and R. Messner, *The Hydrolysis of Cations*, John Wiley & Sons, New York, 1976, p.348.
24 R. A. Waldo, *Microbeam Anal.*, 1988, 310.
25 Joint Committee on Powder Diffraction Standards, Card 6–354, Swarthmore, PA.

Paper 7/06471C; *Received* 4*th September*, 1997